DOI 10.1002/mnfr.201100659 *Mol. Nutr. Food Res.* 2012, *56*, 610–621

RESEARCH ARTICLE

Cyanidin-3-O-β-glucoside upregulates hepatic cholesterol 7α-hydroxylase expression and reduces hypercholesterolemia in mice

Dongliang Wang[1], Min Xia[1], Song Gao[2,3], Dan Li[1], Yuan Zhang[1], Tianru Jin[1,2,3] and Wenhua Ling[1,4]

[1] Department of Nutrition, School of Public Health, Sun Yat-Sen University, Guangzhou, P. R. China
[2] Department of Physiology, University of Toronto, Toronto, Canada
[3] Department of Medicine, University of Toronto, Toronto, Canada
[4] Guangdong Provincial Key Laboratory of Food, Nutrition and Health, Guangzhou, P. R. China

Received: September 28, 2011
Revised: November 11, 2011
Accepted: December 2, 2011

Scope: Although previous studies have shown that consumption of anthocyanin extract from plant foods reduces hypercholesterolemia and the severity of atherosclerosis in different animal models, the mechanisms of these actions remained unclear. This study investigated whether pure anthocyanin inhibit atherosclerosis development and reduce hypercholesterolemia in the apolipoprotein E (ApoE)-deficient mice through enhancement of fecal bile acid excretion, a critical pathway for eliminating circulation cholesterol from the body.

Methods and results: Five-week-old male ApoE-deficient mice were fed the AIN-93G diet supplemented with or without cyanidin-3-*O*-β-glucoside (0.06% w/w) for 12 weeks. Results showed that cyanidin-3-*O*-β-glucoside consumption inhibited the formation of aortic sinus plaque and reduced hypercholesterolemia, along with promoted fecal bile acid excretion and upregulated hepatic cholesterol 7a-hydroxylase expression (CYP7A1). In mouse primary hepatocytes, cyanidin-3-*O*-β-glucoside treatment increased bile acid synthesis and CYP7A1 expression in a liver X receptor alpha (LXRα)-)-dependent manner. Scintillation proximity and time-resolved fluorescence resonance energy transfer assays revealed that cyanidin-3-*O*-β-glucoside functions as an agonist of LXRα.

Conclusion: Our results indicate that the hypocholesterolemic activity of cyanidin-3-*O*-β-glucoside was, at least in part, mediated by activating the potential LXRα-CYP7A1-bile acid excretion pathway, thus contributing to the antiatherogenic effect of cyanidin-3-*O*-β-glucoside. Importantly, cyanidin-3-*O*-β-glucoside could activate LXRα in an agonist-dependent manner.

Keywords:
Anthocyanin / Atherosclerosis / Cholesterol / CYP7A1 / Liver X receptor

Correspondence: Dr. Wenhua Ling, Department of Nutrition, School of Public Health, Sun Yat-Sen University, Guangzhou 510080, P. R. China
E-mail: lingwh@mail.sysu.edu.cn
Fax: +86-20-87330446

Abbreviations: 24(S),25-EC, 24(S),25-epoxycholeserol; **β-gal**, β-galactosidase; **ApoE**, apolipoprotein E; **ApoA-I**, apolipoprotein A-I; **ASCVD**, atherosclerotic cardiovascular disease; **CYP7A1**, cholesterol 7α-hydroxylase expression; **Cy-3-G**, cyanidin-3-*O*-β-glucoside; **GGPP**, geranylgeranyl pyrophosphate; **LBD**, ligand-binding domain; **LUC**, luciferase; **LXRα**, liver X receptor alpha; **siRNA**, small interfering RNA; **SPA**, scintillation proximity assay; **TC**, total cholesterol; **TG**, triglyceride; **TR-FRET**, time-resolved fluorescence resonance energy transfer

1 Introduction

Atherosclerotic cardiovascular disease (ASCVD) is the leading cause of death in most developed countries. Hypercholesterolemia is a well-known risk factor for ASCVD. Plasma cholesterol homeostasis is regulated by dietary cholesterol intake, cholesterol absorption/excretion, and synthesis [1]. Cholesterol 7α-hydroxylase (CYP7A1) is a liver-specific cytochrome P450 isozyme of the CYP7A family that catalyses the rate-limiting step in the classic pathway of bile acid synthesis [2]. Conversion of cholesterol to bile acid in the liver is the most important pathway for elimination of cholesterol from the body. Enhancement of

cholesterol excretion in the form of bile acid is thus an attractive target to combat hypercholesterolemia and atherosclerosis development [3].

Flavonoids represent a diverse range of polyphenolic compounds that occur naturally in plant foods. Extensive epidemiological studies have shown that dietary flavonoids consumption is inversely associated with the incidence of atherosclerotic diseases [4]. Experimental animal work has also shown the antiatherogenic property of flavonoids from various sources [5]. Furthermore, both in vitro cell culture studies and experimental animal work have been utilized to explore mechanisms underlying the protective effect of these natural agents [6]. Among the potential mechanisms revealed to date, maintaining plasma cholesterol homeostasis potential of flavonoids has drawn our attention intensively [7–10].

Anthocyanin, the flavonoid consumed by human beings the most [11], is abundant in various colorful fruits, vegetables, red wine, and grains [12]. Anthocyanin has been shown to possess various biological activities [5]. Our previous studies have demonstrated that outer layer fraction of black rice rich in anthocyanin [13] or anthocyanin extract from black rice [14] inhibits atherosclerosis development partially via its hypocholesterolemic property in apolipoprotein E (ApoE)-deficient mouse model. Other groups also reported that anthocyanin extract from black soybean [15] or blueberries [16] possesses hypocholesterolemic activity. However, the hypocholesterolemic mechanism of anthocyanin is poorly understood.

In the present study, we reported that in the ApoE-deficient mouse model, individual cyanidin-3-*O*-β-glucoside (Cy-3-G) consumption for 12 weeks significantly inhibits formation of early atherosclerosis and decreases plasma total cholesterol (TC) levels. More importantly, we showed for the first time that the hypocholesterolemic potential of Cy-3-G is achieved partially via the increment of fecal bile acid excretion arising from activating the potential liver X receptor alpha (LXRα)-CYP7A1-bile acid excretion pathway.

2 Materials and methods

2.1 Chemicals

Cy-3-G (purity ≥98%) was kindly provided by Polyphenol AS (Sandnes, Norway). Antibodies specific for CYP7A1 and LXRα were purchased from Santa Cruz Biotechnology (Santa Cruz, CA). The β-actin antibody was from Cell Signaling Technology (Danvers, MA). Trizol reagent, M-MLV reverse transcriptase, and polymerase chain reaction (PCR) Mast Mix were purchased from Invitrogen Life Technology (Carlsbad, CA). All other chemicals, unless otherwise indicated, were purchased from Sigma-Aldrich (St. Louis, MO).

2.2 Mice and procedures

ApoE-deficient mice were provided by Jackson Laboratories (Sacramento, CA). Mice were bred and maintained in our pathogen-free facility. Five-week-old male ApoE-deficient mice were individually housed in metabolic cages and fed an AIN-93G phenolic-free diet (control group, $n = 13$) or an AIN-93G diet supplemented with Cy-3-G (0.06% w/w) (Cy-3-G group, $n = 13$) for 12 weeks. The dose of Cy-3-G (0.06% w/w) is approximately 100 mg (kg of body weight)$^{-1}$ day^{-1} that is comparable to estimated concentrations of anthocyanins (130 mg (kg of body weight)$^{-1}$ day^{-1}) used in the study using anthocyanin extract from black rice [14]. The compositions of the experimental diets were given in Supporting Information Table 1. Feces were collected for three consecutive days prior to sacrifice for measurement of bile acid and cholesterol. At the end of the experiment, mice were fasted for 4 h and anaesthetized using diethyl ether. Heparinized plasma samples were collected and kept at −80°C prior to use. The livers, aortas, and hearts were removed and weighed, frozen in liquid nitrogen, and then stored at −80°C for further analyses. All the animal procedures were approved by the Animal Care and User Committee of Sun Yat-Sen University.

2.3 Quantification of atherosclerosis

Method for measurement of atherosclerotic lesions at the aortic sinus has been previously described [17]. Briefly, the upper sections of the hearts were embedded in OCT compound and frozen at −20°C. Every other section (10 μm thick) throughout the aortic sinus (400 μm) was taken for analysis. Cryostat sections were evaluated for fatty streak lesions after staining with Oil red O using computer-assisted imaging and the Optimas Image Analysis software package (Bioscan Inc., Edmonds, WA).

2.4 Plasma, liver, and aorta lipid parameters

The concentrations of plasma TC, triglyceride (TG), and high-density lipoprotein-cholesterol (HDL-C) were measured using the corresponding commercial enzyme kits (Biosino, Beijing, China) on a Biosystem automatic biochemistry analyzer (Madrid, Spain). The level of non-HDL-C was calculated as TC minus HDL-C. Plasma levels of apolipoprotein A-I (ApoA-I) were quantified by a mouse ApoA-I enzyme-linked immunosorbent kit (Cusabio Biotech Co., Ltd, Wuhan, P. R. China) following the manufacturer's instructions. Total lipids were extracted from tissue (liver and aorta) samples according to the method of Bligh and Dyer [18]. After evaporation to dryness under a stream of nitrogen, the lipid extracts were resuspended in a solution of 90% isopropanol, 10% Triton X-100. TC and TG contents were then quantified using the corresponding commercial enzyme kits (Biosino, Beijing, China) as described above.

2.5 Measurement of fecal bile acid and cholesterol

Bile acid and cholesterol were extracted from fecal samples as described by Batta et al. [19]. The concentrations of fecal bile acid and cholesterol were determined by a total bile acid (TBA) assay kit (Sekisui Medical Co., Ltd, Tokyo, Japan) and a cholesterol quantification kit (BioVision, Mountain View, CA), respectively. The daily excretion rates of both bile acid and cholesterol are expressed as micromole/day per 100 g of body weight [20].

2.6 Isolation and culture of mouse primary hepatocytes

Primary hepatocytes were isolated from mice using a modified two-step perfusion method using Liver Perfusion Media and Liver Digest Buffer (Invitrogen, Carlsbad, CA) [21]. The cells were plated onto 60-mm mouse collagen IV-coated dishes at a density of 1.2×10^6 viable cells/dish in serum-free Williams E medium supplemented with thyroxine (1 μmol/L), dexamethasone (0.1 μmol/L), and insulin (0.02 nmol/L). The hepatocytes were used only if they were greater than 90% viable as assessed by trypan blue exclusion. The purity of hepatocytes was over 99% as nonparenchymal cells judged by their size (<10 μm diameter) and morphology (nonpolygonal or stellate) [22] were less than 1%.

2.7 Western blotting

Aliquots (40 μg) of cell lysates were separated by sodium dodecyl sulfate (SDS)-polyacrylamide gel electrophoresis. Method for Western blotting has been previously described [23]. Hepatic microsomes from liver tissue samples were isolated as described by Zanger et al. [24] for the analysis of CYP7A1 protein levels. Specific antibodies used included CYP7A1, LXRα, and β-actin. Anti-β-actin was used for equal protein loading.

2.8 Quantitative real-time RT-PCR

Methods for RNA extraction and quantitative real-time reverse transcriptase-PCR (qRT-PCR) have been previously described in our previous publications [25]. The primer sequences are listed in Supporting Information Table 2. β-actin mRNA was used as the internal control.

2.9 Bile acid assay

Hepatocyte culture medium was collected for the analysis of TBA. TBA in culture medium was partially purified with Sep-Pak C18 cartridge (Walters, Milford, MA) as described by Li et al. [26], and then quantified as described above.

2.10 Construction of the mouse CYP7A1-luciferase (LUC) reporter plasmids

The 0.9 kb mouse CYP7A1 gene 5¢ flanking region (−835 to +55 bp) was obtained by PCR against C57BL6 mouse tail DNA with a pair of primers (Supporting Information Table 3). The PCR product was inserted into the TA cloning vector followed by DNA sequencing verification (NC_000070.5). This DNA fragment was then subcloned into a promoterless p-BLUC LUC plasmid [27] and designated as −835 bp CYP7A1-LUC. Two deletion constructs, designated as −83 bp CYP7A1-LUC (with the LXR binding site) and −55 bp CYP7A1-LUC (without the LXR binding site), were obtained by a further subcloning procedure, utilizing the two new forward primers (Supporting Information Table 3).

2.11 Transient transfection and reporter gene assays

Mouse primary hepatocytes were transfected with 1 μg of CYP7A1-LUC reporter plasmid and 0.5 μg of β-galactosidase (β-gal) control vector (Promega, Madison, WI) using lipofectamine 2000 (Invitrogen) following the manufacturer's instructions. Sixteen hours after transfection, cells were treated with Cy-3-G for 24 h. LUC and β-gal activities were analyzed in cell lysates.

2.12 Scintillation proximity assay

Scintillation proximity assay (SPA) was performed to identify ligands of LXRα with the method of Janowski et al. [28] Briefly, scintillant-filled beads (GE Healthcare, Buckinghamshire, UK) precoated with polylysine to permit protein binding were diluted in SPA buffer to a final concentration of 5 mg/mL. Binding assays were performed in 384-well plates in 20 μL containing beads (0.2 mg per well) and His-LXRα ligand-binding domain (LBD) (120 ng per well, Roche Diagnostics, Indianapolis, IN). ^{3}H-24(S),25-epoxycholeserol (24(S),25-EC) (PerkinElmer, Boston, MA) was added to wells at a single concentration of 25 nmol/L. The amount of protein used did not deplete ligand concentrations. All competition binding assays for 24(S),25-EC or Cy-3-G were tested at concentration ranging from 3 nmol/L to 50 μmol/L. Plates were shaken at 25°C for 3 h, and radioactivity was then measured in a Packard Topcount at 1 min per well. All concentrations were assayed in triplicate. Wells devoid of competitor represented 100% binding. Nonspecific binding was quantified by leaving His-LXRα LBD out of the SPA reaction. Competition curves were generated by nonlinear regression analysis using GraphPad™ Prism® 5.0 (GraphPad Software Inc., San Diego, CA) and the apparent equilibrium dissociation constants (K_i values) were determined by using a method described by DeBlasi and colleagues [29].

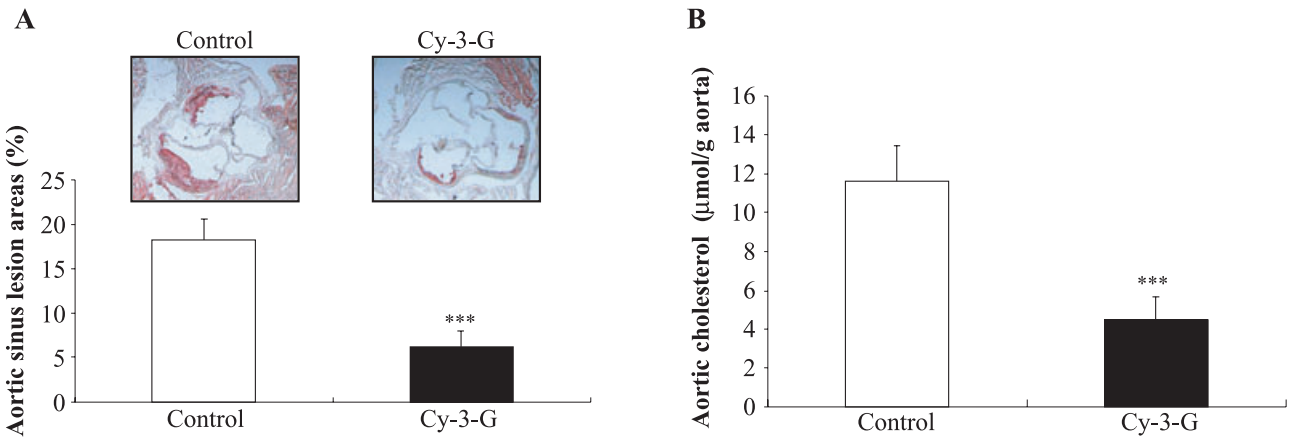

Figure 1. Cy-3-G consumption inhibits atherosclerosis development in ApoE-deficient mice. Mice were fed with the AIN-93G diet supplemented with or without 0.06% Cy-3-G (w/w) for 12 wk. (A) Representative cryostat sections of aortic sinus (40×) stained with Oil Red O. (Top panel) Representative images. (Bottom panel) Quantitative analysis of panel A. (B) Lipids were extracted for the measurement of aortic cholesterol. For bottom panel A and panel B, results are mean ± SEM ($n = 13$ per group). ***$p < 0.001$.

2.13 Time-resolved fluorescence resonance energy transfer (TR-FRET) assay

The TR-FRET LXRα coactivator assay kit (Invitrogen) was used to identify agonists of LXRα. In these cell-free assays, agonists are identified by their ability to bind LXRα LBD and induce a conformational change that results in recruitment of a fluorescein-labeled coactivator peptide. Briefly, glutathione *S*-transferase (GST)-LXRα LBD was labeled with terbium (Tb)-anti-GST antibody, and coactivator TRAP220/DRIP-2 peptides were labeled with fluorescein. Cy-3-G or 24(S),25-EC ranging from 3 nmol/L to 100 μmol/L was incubated in the assay buffer with 5 nmol/L GST-LXRα LBD, 10 nmol/L Tb-anti-GST antibody, and 250 nmol/L of fluorescein-TRAP220/DRIP-2 peptide for 2 h at room temperature. At the end of the incubation period, the 520/495 TR-FRET ratio was measured with a PerkinElmer Envision fluorescent plate reader with time-resolved fluorescence (TRF) laser excitation using the following filter set: excitation 340 nm, emission 495 nm, and emission 520 nm. A 100-μs delay followed by a 200-μs integration time was used to collect the time-resolved signal. Dose responses curves of Cy-3-G or 24(S),25-EC were generated using a sigmoidal dose response (variable slope) equation in GraphPad™ Prism® 5.0 allowing calculation of EC_{50} values.

2.14 LXRα protein knockdown

LXRα protein expression was knocked down by transfection of mouse LXRα small interfering RNA (siRNA) duplex with mouse primary hepatocytes. A nonrelated, scrambled siRNA was used as a control. All siRNA oligos were designed and synthesized by Santa Cruz (Santa Cruz Biotechnology). The transfection assay was performed as described in our previous publications [30]. At selected time points after transfection, cells were lysed and subjected to Western blotting analysis to evaluate intracellular LXRα protein levels.

2.15 Statistical analysis

Results are presented as the mean ± standard error of the mean (SEM). Data were statistically analyzed with either Student's *t*-test (two tailed) or one-way ANOVA coupled with the Student–Newman–Keuls multiple comparison test. Differences were considered significant if $p < 0.05$.

3 Results

3.1 Cy-3-G consumption inhibits atherosclerotic plaque formation in ApoE-deficient mice

Previously, we demonstrated that anthocyanin extract from black rice remarkably inhibits atherosclerosis development in the ApoE-deficient mouse model [14]. Since Cy-3-G is the major form of anthocyanin in anthocyanin extract from black rice [14], ApoE-deficient mice were fed the AIN-93G diet with or without Cy-3-G (0.06% w/w) for 12 weeks. Compared with the control group, mice in the Cy-3-G group showed not only a 66% reduction of the aortic sinus plaque area (Fig. 1A), but also a 61% reduction of the aortic cholesterol accumulation (Fig. 1B), the latter being an alternate index for the severity of atherosclerosis [31].

3.2 Cy-3-G consumption improves lipid profile in plasma and liver in ApoE-deficient mice

Cy-3-G consumption for 12 weeks significantly decreased plasma TC, TG, and non-HDL-C levels, and increased plasma HDL-C and ApoA-I concentrations (Table 1). Moreover, total

Table 1. Effect of Cy-3-G consumption on plasma and liver lipid concentrations, and plasma ApoA-I levels in ApoE-deficient mice

Parameters	Control	Cy-3-G
Plasma lipids and ApoA-I		
TC (mmol/L)	14.24 ± 1.36	10.27 ± 1.15[a)]
TG (mmol/L)	1.91 ± 0.10	1.26 ± 0.08[a)]
HDL-C (mmol/L)	0.55 ± 0.08	0.90 ± 0.11[a)]
non-HDL-C (mmol/L)	13.68 ± 1.51	9.36 ± 1.36[a)]
ApoA-I (mg/dL)	21.44 ± 1.78	30.31 ± 2.60[a)]
Liver lipids (mg/g liver)		
Total cholesterol	63.5 ± 4.3	49.2 ± 3.7[a)]
Total triglyceride	7.2 ± 0.9	6.5 ± 0.8

Data are mean ± SEM ($n = 13$ per group).
a) Means in a row with different letters differ significantly ($p < 0.05$).

cholesterol in the liver decreased significantly in the Cy-3-G group compared with the control group (Table 1). No significant differences in hepatic total TG levels were seen between the Cy-3-G and control group (Table 1).

3.3 Cy-3-G consumption promotes fecal bile acid output and upregulates hepatic CYP7A1 expression in ApoE-deficient mice

To test the possibility whether the hypocholesterolemic activity of Cy-3-G is associated with enhancement of bile acid excretion, we determined the levels of fecal bile acid and cholesterol in the experimental and control animals. As shown in Figure 2A, fecal bile acid but not cholesterol output significantly increased in the Cy-3-G group mice than the control group animals. Increased excretion of bile acid in feces upon Cy-3-G consumption indicated that hepatic bile salt synthesis might be increased. The rate-limiting enzyme for the classic pathway of bile acid synthesis in the liver is CYP7A1 [2]. The qRT-PCR and Western blot analyses demonstrated that Cy-3-G consumption significantly increased mRNA and protein expression of hepatic CYP7A1 in the ApoE-deficient mice (Fig. 2B and C).

3.4 Cy-3-G increases bile acid synthesis and upregulates CYP7A1 expression at the transcriptional level in mouse primary hepatocytes

To verify the effect of Cy-3-G on hepatic CYP7A1 expression in vitro, we isolated primary hepatocytes from ApoE-deficient mice (male, aged 6–8 weeks) as the cell model. Incubation of mouse primary hepatocytes with Cy-3-G (1.0–50 μM) for 24 h significantly promoted bile acid synthesis (Fig. 3A). This promotion was associated with the increase of CYP7A1 protein (Fig. 3B) and mRNA (Fig. 3C) expression.

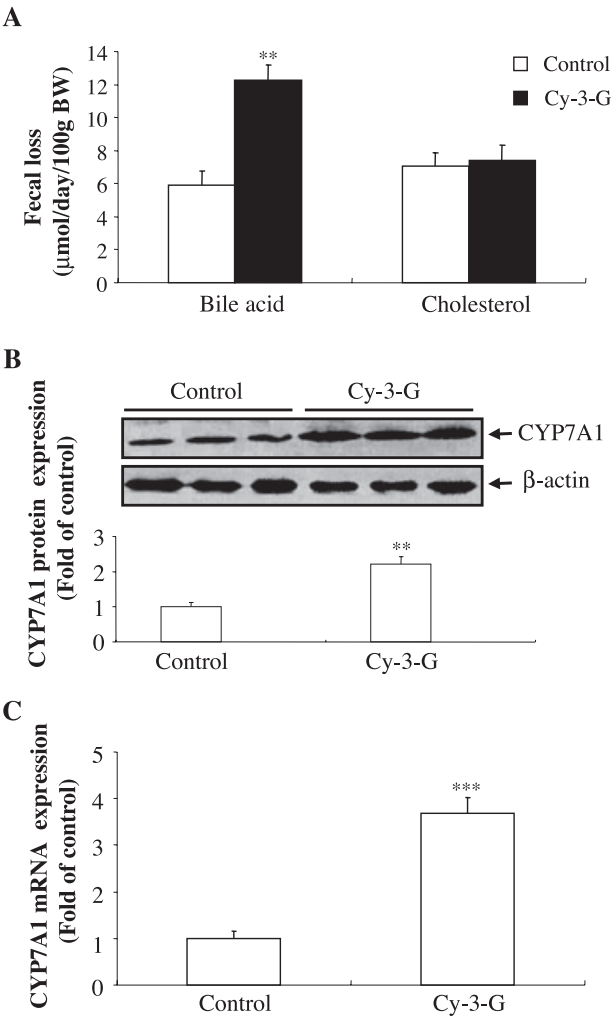

Figure 2. Cy-3-G consumption increases fecal bile acid excretion and upregulates hepatic CYP7A1 expression in ApoE-deficient mice. Mice were fed with the AIN-93G diet supplemented with or without 0.06% Cy-3-G (w/w) for 12 weeks. (A) Fecal bile acid and cholesterol output. Results are mean ± SEM ($n = 13$ per group). $^{**}p < 0.01$. (B) Detection hepatic CYP7A1 protein expression levels by Western blotting. (Top panel) Representative blot of six independent experiments. (Bottom panel) Quantitative analysis of panel B. (C) Detection of hepatic CYP7A1 mRNA expression levels by qRT-PCR. For bottom panel B and panel C, results are mean ± SEM ($n = 6$ per group). $^{***}p < 0.001$, $^{**}p < 0.01$.

To determine whether the elevation of CYP7A1 mRNA level by Cy-3-G treatment was mediated by the CYP7A1 promoter, we constructed a mouse CYP7A1 promoter LUC fusion gene construct (−835 bp CYP7A1-LUC), and found that Cy-3-G (1.0–50 μM) significantly increased the expression of −835 bp CYP7A1-LUC in mouse primary hepatocytes (Fig. 3D). These data imply that Cy-3-G induces CYP7A1 gene expression at the transcriptional level, thus leading to enhancement of bile acid synthesis.

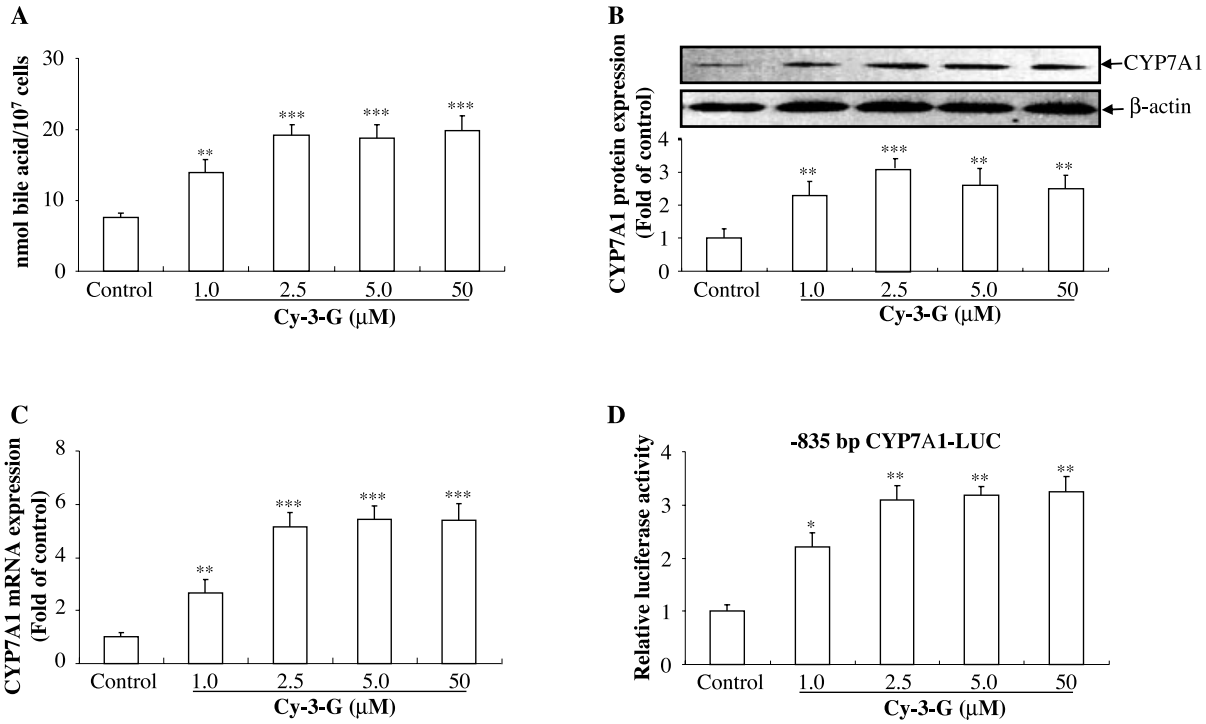

Figure 3. Cy-3-G promotes bile acid synthesis and CYP7A1 expression at transcriptional level in mouse primary hepatocytes. Hepatocytes were treated with indicated concentrations of Cy-3-G for 24 h. (A) Cell culture medium was obtained for the measurement of bile acid levels. Results are mean ± SEM ($n = 6$ per group). ***$p < 0.001$, **$p < 0.01$. (B and C) The effect of Cy-3-G on CYP7A1 expression was assessed by Western blotting (B) and qRT-PCR (C). Top panel B is a representative image of three independent experiments. (Bottom panel B) Quantitative analysis of panel B. Results are mean ± SEM ($n = 3$ per group). ***$p < 0.001$, **$p < 0.01$. (D) Cy-3-G increased the expression of –835 bp CYP7α1-LUC. Hepatocytes cotransfected with the –835 bp CYP7A1-LUC reporter plasmids and β-galactosidase plasmids were treated with Cy-3-G at the indicated concentrations for 24 h. Luciferase activity was then measured and normalized using the β-galactosidase activity. Results are mean ± SEM relative to the untreated control cells (assigned a value of 1.0) ($n = 6$). **$p < 0.01$, *$p < 0.05$.

3.5 The stimulatory effects of Cy-3-G on bile acid synthesis and CYP7A1 expression are dependent on LXRα in mouse primary hepatocytes

It is known that CYP7A1 is transcriptionally regulated by LXRα [32]. We then asked whether LXRα is required for the increment of CYP7A1 promoter activity by Cy-3-G. To test this, we have first of all, made two additional CYP7A1-LUC reporter gene constructs, namely, −83 bp CYP7A1-LUC, with the LXRα binding site; and −55 bp CYP7A1-LUC, without the LXRα binding site (Fig. 4A). We found that Cy-3-G stimulated the expression of −83 bp CYP7A1-LUC (Fig. 4B) but not −55 bp CYP7A1-LUC (Fig. 4C) in mouse primary hepatocytes. This observation suggests that the LXRα binding motif on CYP7A1 promoter is required for Cy-3-G in stimulating its transcription.

To further verify the role of LXRα in inducing bile acid synthesis and expression of CYP7A1 by Cy-3-G treatment, we employed an siRNA knockdown approach. As expected, LXRα siRNA transfection significantly reduced LXRα expression level without affecting the control protein expression in the mouse primary hepatocytes (Supporting Information Fig. 1), and this silencing effect could last for 72 h. Hepatocytes transfected with LXRα siRNA were then treated with the indicated concentration of Cy-3-G for 24 hours. The results showed that the stimulatory effects of Cy-3-G on the bile acid synthesis (Fig. 5A), CYP7A1 protein (Fig. 5B), and mRNA expression (Fig. 5C) were markedly reduced. Given that LXRα is a ligand-dependent transcriptional factor, we further utilized a known antagonist of LXRα, geranylgeranyl pyrophosphate (GGPP) [33]. The coincubation of mouse primary hepatocytes with GGPP significantly reduced the stimulatory effects of Cy-3-G on the bile acid synthesis (Fig. 5D), CYP7A1 protein (Fig. 5E), and mRNA (Fig. 5F) expression. These data demonstrated that the stimulatory effects of Cy-3-G on bile acid synthesis and CYP7A1 expression depend on the LXRα.

3.6 Cy-3-G activates LXRα in a ligand-dependent manner

Previously, we demonstrated that Cy-3-G increases LXRα expression in murine- and human-derived macrophages

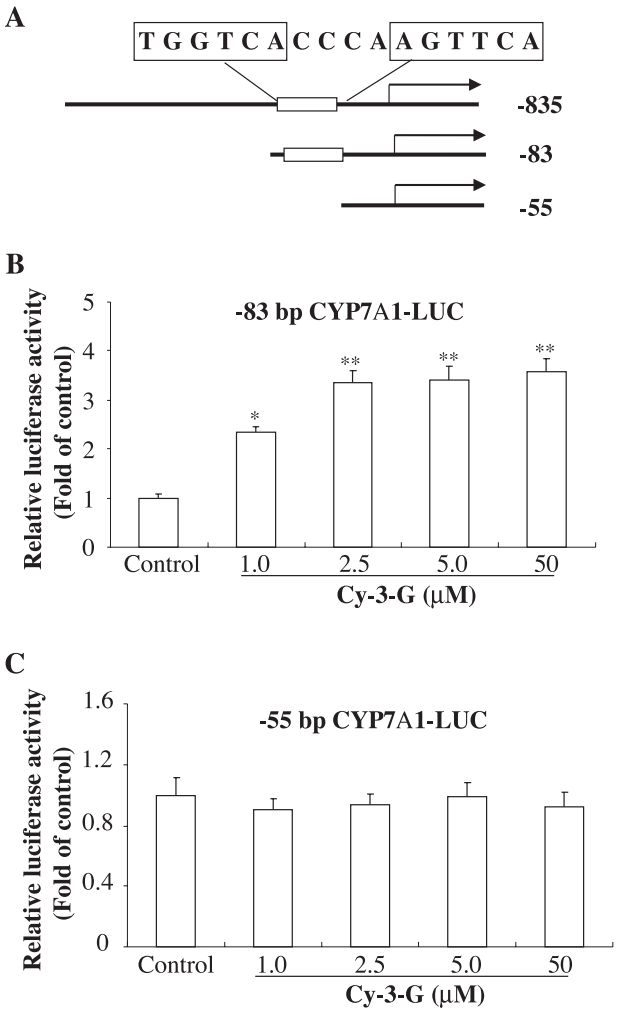

Figure 4. Cy-3-G increased the expression of −83 bp but not −55 bp CYP7A1-LUC in mouse primary hepatocytes. (A) The diagram shows three different CYP7A1-LUC reporter plasmids. Hepatocytes cotransfected with the −83 bp (B) or −55 bp (C) CYP7A1-LUC reporter plasmids and β-galactosidase plasmids were treated with Cy-3-G at the indicated concentration for 24 h. Luciferase activity was then measured and normalized using the β-galactosidase activity. Results are mean ± SEM relative to the untreated control cells (assigned a value of 1.0) ($n = 6$). $^{**}p < 0.01$, $^{*}p < 0.05$.

[34, 35]. Herein, we found that Cy-3-G treatment (1–50 μM) for 24 h or Cy-3-G consumption (0.06% w/w) for 12 wk significantly increased LXRα protein mass in mouse primary hepatocytes and the liver of ApoE-deficient mice (Fig. 6A and 6B), respectively. Given that LXRα is a ligand-activated transcription factor, we further asked whether Cy-3-G could function as a ligand for LXRα. For this purpose, we performed a SPA assay using ^{3}H-24(S),25-EC as the radioligand. As shown in Figure 6C, the endogenous LXRα ligand 24(S),25-EC expectedly displaced ^{3}H-24(S),25-EC from LXRα LBD ($K_i = 265 \pm 9$ nmol/L). When Cy-3-G was added into the system, it directly displaced ^{3}H-24(S),25-EC from LXRα LBD and possessed a high affinity to LXRα LBD ($K_i = 138 \pm 3$ nmol/L). To further characterize the function of binding of Cy-3-G to LXRα LBD, a TR-FRET assay was performed, which evaluates the ability of test compounds to recruit a TRAP220/DRIP-2 coactivator peptide to LXRα LBD. We found that both Cy-3-G and 24(S),25-EC elicited recruitment of coactivator to LXRα LBD in this system (Fig. 6D). The EC_{50} of Cy-3-G and 24(S),25-EC were 3.74 and 2.73 μmol/L, respectively.

4 Discussion

Our results demonstrated the following for the first time: (i) consumption of pure Cy-3-G compound inhibited formation of early atherosclerosis and attenuated hypercholesterolemia in the ApoE-deficient mice; (ii) Cy-3-G consumption promoted hepatic CYP7A1 expression and fecal bile acid output; (iii) Cy-3-G treatment enhanced bile acid synthesis arising from upregulation of CYP7A1 expression through activating LXRα partially in an agonist-dependent manner in mouse primary hepatocytes.

As mentioned above, hypercholesterolemia has been identified as a major risk factor for ASCVD, and several therapeutic approaches have been utilized to reduce the rate of morbidity and mortality associated with hypercholesterolemia and atherosclerosis. For example, inhibitors of cholesterol synthesis (statins) [36] and absorption (ezetimibe) [37] have shown several beneficial effects related to their cholesterol-lowering activity. However, other approaches in lowering the plasma cholesterol are needed in subjects who are resistant to statins treatment or highly sensitive to statins side effects. Previous studies have shown that anthocyanin extract rich in Cy-3-G reduces plasma cholesterol levels in different animal models [13], implicating that Cy-3-G possesses the hypocholesterolemic potential. In the present study, we clearly showed that Cy-3-G consumption for 12 weeks significantly attenuated hypercholesterolemia in the ApoE-deficient mouse model, which was associated with a reduction of formation of early atherosclerosis. These data suggested that the hypocholesterolemic potential of Cy-3-G may contribute in part to its antiatherogenic effect in the ApoE-deficient mouse model. Abundant data showed that anthocyanin extracts from various sources including black rice [14], bilberry [38], and purple sweet potato [39] have been consistently shown to attenuate inflammation response in the same ApoE-deficient mouse model. Taken together, the potential atheroprotective mechanisms of Cy-3-G observed here may be related to its cholesterol-lowering property and anti-inflammatory activity.

It is known that fecal bile acid excretion is an important mechanism for maintaining plasma cholesterol homeostasis. One important component of the process of fecal bile acid excretion is hepatic CYP7A1. Transgenic overexpression of CYP7A1 in C57BL/6J mice enhances fecal bile acid excretion and reduced cholesterol accumulation in the liver and plasma [40]. Spady et al. [41] reported that adenovirus-mediated

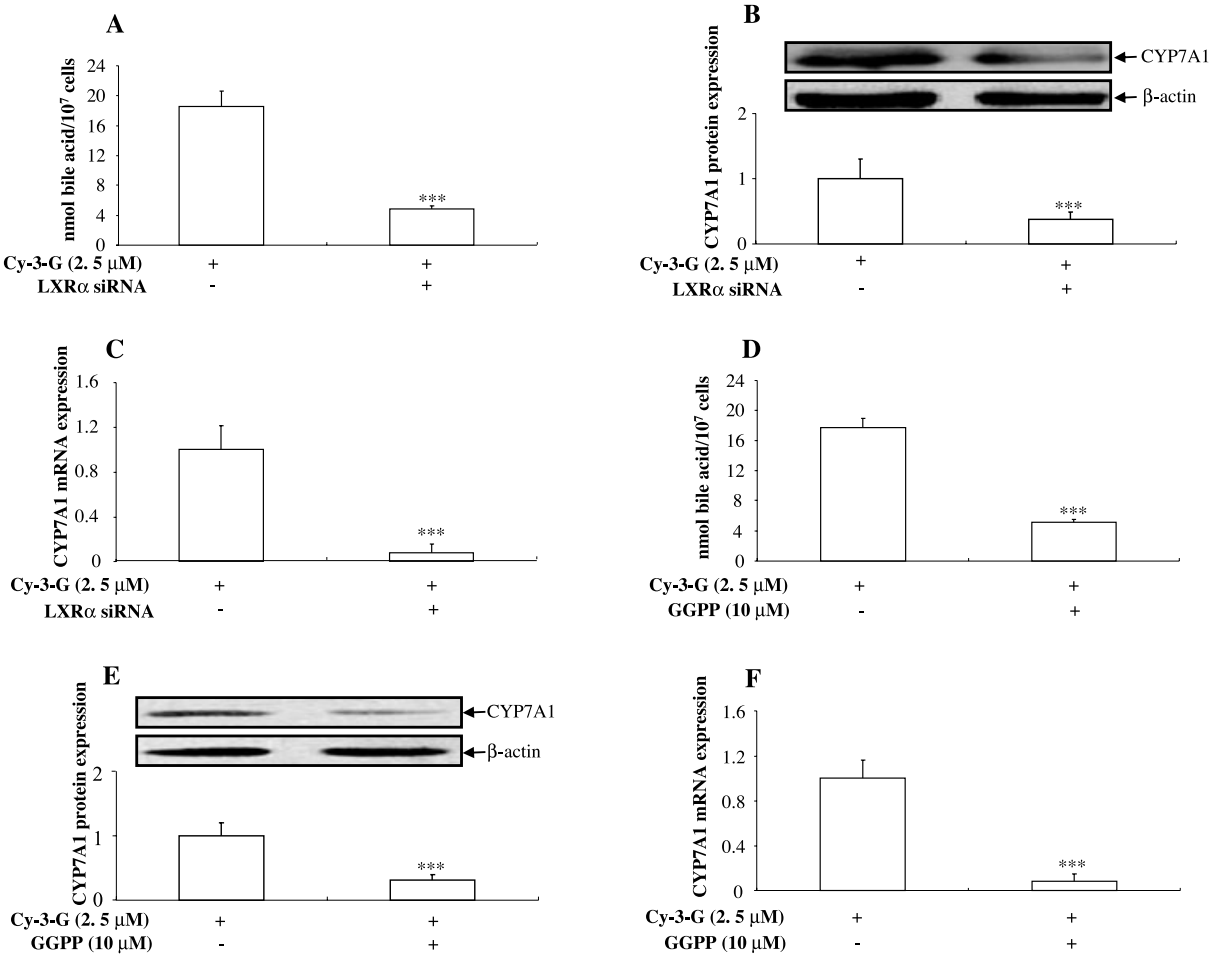

Figure 5. The stimulatory effect of Cy-3-G on bile acid synthesis and CYP7A1 expression requires LXRα in mouse primary hepatocytes. (A–C) LXRα siRNA or control scrambled siRNA-transfected hepatocytes were treated with Cy-3-G (2.5 μM) for 24 h. Cell culture medium was obtained for the measurement of bile acid levels (A). Results are mean ± SEM ($n = 6$ per group). ***$p < 0.001$. CYP7A1 expression was assessed by Western blotting (B) and qRT-PCR (C). Top panel B is a representative image of three independent experiments. (Bottom panel B) Quantitative analysis of panel B. For bottom panel B and panel C, results are mean ± SEM ($n = 3$ per group). ***$p < 0.001$. (E and F) Hepatocytes were treated with Cy-3-G (2.5 μM) for 24 h in the presence or absence of GGPP (10 μM). Bile acid levels in cell culture medium (D), CYP7A1 protein (E) and mRNA (F) expression levels were determined as above. Top panel E is a representative image of three independent experiments. (Bottom panel E) Quantitative analysis of panel E. For bottom panel E and panels D and C, results are mean ± SEM ($n = 3$ per group). ***$p < 0.001$.

overexpression of CYP7A1 in low-density lipoprotein-receptor knockout mice lowers hypercholesterolemia. In contrast, CYP7A1 gene knockout mouse had decreased fecal bile acid excretion and hypercholesterolemia [42]. In the current work, we demonstrated that Cy-3-G consumption for 12 weeks increased fecal bile acid excretion and hepatic CYP7A1 mass, as well as reduced hepatic cholesterol levels in the ApoE-deficient mice. Similarly, Mauray et al. reported that anthocyanin extract from bilberry consumption for 2 weeks induced CYP7A1 gene expression and reduced cholesterol accumulation in the liver of ApoE-deficient mice [43]. Furthermore, we demonstrated that Cy-3-G treatment increased bile acid synthesis and CYP7A1 expression in mouse primary hepatocytes. Hence, potential mechanism for the hypocholesterolemic effect of Cy-3-G was related to the enhancement of fecal bile acid excretion, at least in part, mediated by the increment of hepatic CYP7A1 mass.

CYP7A1 is transcriptionally regulated by multiple transcription factors including LXRα [32]. On the basis of our previous work that Cy-3-G activates LXRα via increasing its protein expression in murine- and human-derived macrophages [34, 35], we hypothesized that the stimulatory effects of Cy-3-G on CYP7A1 gene expression and bile acid synthesis involved in the activation of LXRα in mouse primary hepatocytes. Indeed, reporter gene analyses have shown that the increased activity of CYP7A1 gene promoter by Cy-3-G treatment requires the LXR binding site. Furthermore, using siRNA-mediated protein knockdown methodology and

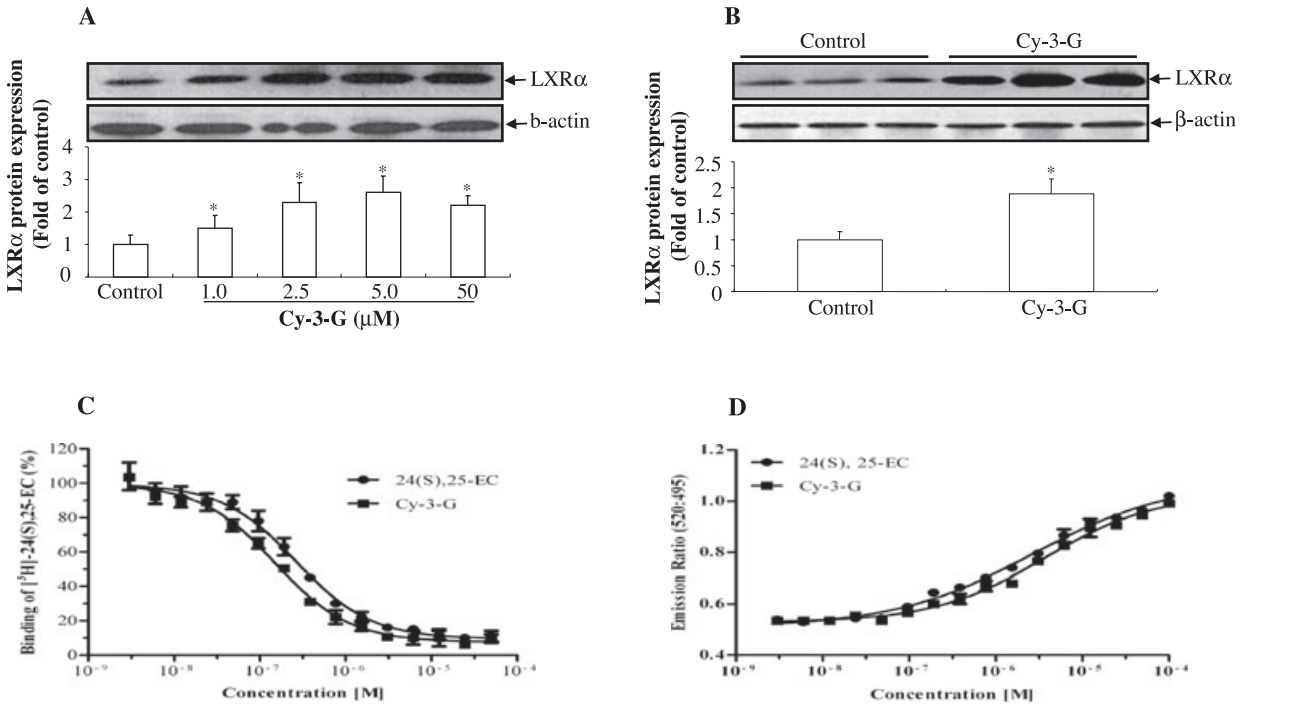

Figure 6. Cy-3-G activates LXRα via increasing its expression and functioning as its agonist. (A) Mouse primary hepatocytes were treated with indicated concentrations of Cy-3-G for 24 h. Whole cell lysates were prepared for Western blotting of LXRα. (Top panel A) Representative blot image of three independent experiments. (Bottom panel A) Quantitative analysis of panel A. For bottom panel A, results are mean ± SEM ($n = 3$ per group). *$p < 0.05$. ApoE-deficient mice were fed with the AIN-93G diet supplemented with or without 0.06% Cy-3-G (w/w) for 12 weeks. Hepatic microsomal protein was then prepared for detecting CYP7A1 expression levels by Western blotting (B). (Top panel B) Representative blot of six independent experiments. (Bottom panel B) Quantitative analysis of panel B. Results are mean ± SEM ($n = 6$ per group). *$p < 0.05$. (C) Cy-3-G directly bound to LXRα LBD. A scintillation proximity assay was performed as described in section Materials and methods. (D) Binding of Cy-3-G to LXRα LBD resulted in TRAP220/DRIP-2 coactivator recruitment. A scintillation proximity assay was performed as described in section Materials and methods. For panels C and D, results are mean ± SEM ($n = 3$ per group).

pharmacological approaches, we elucidated that the positive effects of Cy-3-G on bile acid synthesis and CYP7A1 expression are completely dependent on LXRα activation in mouse primary hepatocytes. Next, we investigated how Cy-3-G activates LXRα. By using two cell-free SPA and TR-FRET assays, we provided evidence for the first time that Cy-3-G serves as an agonist of LXRα with comparable efficiency to an LXRα ligand 24(S),25-EC. Additionally, we have also shown that Cy-3-G treatment or consumption increased the expression of LXRα in mouse primary hepatocytes and ApoE-deficient mouse liver, respectively. Taken together, these data firmly demonstrated that the stimulatory effects of Cy-3-G on CYP7A1 expression and bile acid synthesis depended on LXRα, and Cy-3-G activated LXRα via functioning as an agonist of LXRα and increasing its receptor expression.

It is known that LXRα plays a critical role in a variety of physiological processes including cholesterol metabolism, glucose metabolism, TG synthesis, and inflammation [44]. Activation of LXRα is an effective target to combat metabolic diseases including atherosclerosis [44]. The widely used two synthetic nonsteroidal LXR ligands, GW3965 [45] and T0901317 [46], have been shown to remarkably inhibit atherosclerosis. Unfortunately, the concomitant induction of TG synthesis leads to hypertriglyceridemia and liver steatosis [45, 46], which hampers the implication of those LXRα agonists in humans. Notably, we identified that a new LXRα agonist Cy-3-G could not induce fatty liver and hypertriglyceridemia in the ApoE-deficient mice. It has been recognized that anthocyanins have multiple functions such as antioxidation, inhibition of inflammation, and improvement of lipid metabolism [13, 47]. Very recently, we demonstrated that Cy-3-G consumption promotes TG catabolism via activating lipoprotein lipase in the KK-Ay mice [48]. Thus, Cy-3-G-induced TG catabolism may overcome its stimulatory effect on TG synthesis. Furthermore, there are several reports that treatments of anthocyanin-rich extract from different sources decreased TG accumulation in the plasma or liver of mice [15, 16, 43], which are consistent with our findings.

It has been well known that the bioavailability of anthocyanins in humans and animal models is accompanied by extensive conjugation and metabolism in the intestine and liver [49], indicating that either parent anthocyanins or their

metabolites or both are contributed to these in vivo biological effects. Anthocyanins have been shown to be transformed into three main types of metabolites: glucuronidation, sulfation, and methylation in vivo [50]. However, several studies have indicated that the above metabolites are less active than these parent anthocyanins in biological effects [51]. Thus, our current data suggested that intact Cy-3-G is the major contributor for the stimulatory effect on hepatic CYP7A1 expression in the ApoE-deficient mouse model. The present in vitro cell culture studies also revealed that Cy-3-G at low dose of 1 μM that is comparable to the physiological concentrations of anthocyanins in plasma of mice [25] and human [52], upregulated CYP7A1 expression. Recently, some studies have shown that protocatechuic acid, a potential gut microbiota metabolite of Cy-3-G, possesses similar biological effects with its parent Cy-3-G such as the insulin-like [53] and antimonocyte/macrophage infiltration activities [25]. Thus, there is a possibility that the positive effect of Cy-3-G on hepatic CYP7A1 expression in vivo could be partially ascribed to protocatechuic acid. This interesting hypothesis deserves future studies.

In summary, the present study has clearly shown that Cy-3-G possesses the antiatherogenic and hypocholesterolemic effects in the ApoE-deficient mouse model. Mechanistically, the hypocholesterolemic effect of Cy-3-G may be through activating the potential LXRα-CYP7A1-bile acid excretion pathway in vivo. More importantly, we demonstrated for the first time that Cy-3-G could activate LXRα in an agonist-dependent manner.

This work was supported by grants from the National Natural Science Foundation of China (30730079) and the Joint project of NSFC, China-CIHR, Canada, 2010-2012.

The authors have declared no conflict of interest.

5 References

[1] Gylling, H., Cholesterol metabolism and its implications for therapeutic interventions in patients with hypercholesterolaemia. *Int. J. Clin. Pract.* 2004, *58*, 859–866.

[2] Pikuleva, I. A., Cholesterol-metabolizing cytochromes P450. *Drug Metab. Dispos.* 2006, *34*, 513–520.

[3] Luoma, P. V., Cytochrome P450 and gene activation—from pharmacology to cholesterol elimination and regression of atherosclerosis. *Eur. J. Clin. Pharmacol.* 2008, *64*, 841–850.

[4] Mink, P. J., Scrafford, C. G., Barraj, L. M., Harnack, L. et al., Flavonoid intake and cardiovascular disease mortality: a prospective study in postmenopausal women. *Am. J. Clin. Nutr.* 2007, *85*, 895–909.

[5] Basu, A., Rhone, M., Lyons, T. J., Berries: emerging impact on cardiovascular health. *Nutr. Rev.* 2010, *68*, 168–177.

[6] Curin, Y., Andriantsitohaina, R., Polyphenols as potential therapeutical agents against cardiovascular diseases. *Pharmacol. Rep.* 2005, *57* Suppl, 97–107.

[7] Jiao, R., Zhang, Z., Yu, H., Huang, Y. et al., Hypocholesterolemic activity of grape seed proanthocyanidin is mediated by enhancement of bile acid excretion and upregulation of CYP7A1. *J. Nutr. Biochem.* 2010, *21*, 1134–1139.

[8] Koo, S. I., Noh, S. K., Green tea as inhibitor of the intestinal absorption of lipids: potential mechanism for its lipid-lowering effect. *J. Nutr. Biochem.* 2007, *18*, 179–183.

[9] Mulvihill, E. E., Allister, E. M., Sutherland, B. G., Telford, D. E. et al., Naringenin prevents dyslipidemia, apolipoprotein B overproduction, and hyperinsulinemia in LDL receptor-null mice with diet-induced insulin resistance. *Diabetes* 2009, *58*, 2198–2210.

[10] Xiao, C. W., Mei, J., Wood, C. M., Effect of soy proteins and isoflavones on lipid metabolism and involved gene expression. *Front Biosci.* 2008, *13*, 2660–2673.

[11] Hertog, M. G., Hollman, P. C., Katan, M. B., Kromhout, D., Intake of potentially anticarcinogenic flavonoids and their determinants in adults in The Netherlands. *Nutr. Cancer* 1993, *20*, 21–29.

[12] Manach, C., Scalbert, A., Morand, C., Remesy, C. et al., Polyphenols: food sources and bioavailability. *Am. J. Clin. Nutr.* 2004, *79*, 727–747.

[13] Xia, M., Ling, W. H., Ma, J., Kitts, D. D. et al., Supplementation of diets with the black rice pigment fraction attenuates atherosclerotic plaque formation in apolipoprotein e deficient mice. *J. Nutr.* 2003, *133*, 744–751.

[14] Xia, X., Ling, W., Ma, J., Xia, M. et al., An anthocyanin-rich extract from black rice enhances atherosclerotic plaque stabilization in apolipoprotein E-deficient mice. *J. Nutr.* 2006, *136*, 2220–2225.

[15] Kwon, S. H., Ahn, I. S., Kim, S. O., Kong, C. S. et al., Anti-obesity and hypolipidemic effects of black soybean anthocyanins. *J. Med. Food* 2007, *10*, 552–556.

[16] Prior, R. L., Wu, X., Gu, L., Hager, T. et al., Purified berry anthocyanins but not whole berries normalize lipid parameters in mice fed an obesogenic high fat diet. *Mol. Nutr. Food Res.* 2009, *53*, 1406–1418.

[17] Wang, D., Wei, X., Yan, X., Jin, T. et al., Protocatechuic acid, a metabolite of anthocyanins, inhibits monocyte adhesion and reduces atherosclerosis in apolipoprotein E-deficient mice. *J. Agric. Food Chem.* 2010, *58*, 12722–12728.

[18] Iverson, S. J., Lang, S. L., Cooper, M. H., Comparison of the Bligh and Dyer and Folch methods for total lipid determination in a broad range of marine tissue. *Lipids* 2001, *36*, 1283–1287.

[19] Batta, A. K., Salen, G., Rapole, K. R., Batta, M. et al., Highly simplified method for gas-liquid chromatographic quantitation of bile acids and sterols in human stool. *J. Lipid Res.* 1999, *40*, 1148–1154.

[20] Alam, K., Meidell, R. S., Spady, D. K., Effect of up-regulating individual steps in the reverse cholesterol transport pathway on reverse cholesterol transport in normolipidemic mice. *J. Biol. Chem.* 2001, *276*, 15641–15649.

[21] Seglen, P. O., Preparation of isolated rat liver cells. *Methods Cell Biol.* 1976, *13*, 29–83.

[22] Khetani, S. R., Szulgit, G., Del Rio, J. A., Barlow, C. et al., Exploring interactions between rat hepatocytes and nonparenchymal cells using gene expression profiling. *Hepatology* 2004, *40*, 545–554.

[23] Guo, H., Ling, W., Wang, Q., Liu, C. et al., Cyanidin 3-glucoside protects 3T3-L1 adipocytes against H2O2- or TNF-alpha-induced insulin resistance by inhibiting c-Jun NH2-terminal kinase activation. *Biochem. Pharmacol.* 2008, *75*, 1393–1401.

[24] Zanger, U. M., Vilbois, F., Hardwick, J. P., Meyer, U. A., Absence of hepatic cytochrome P450bufl causes genetically deficient debrisoquine oxidation in man. *Biochemistry* 1988, *27*, 5447–5454.

[25] Wang, D., Zou, T., Yang, Y., Yan, X. et al., Cyanidin-3-O-beta-glucoside with the aid of its metabolite protocatechuic acid, reduces monocyte infiltration in apolipoprotein E-deficient mice. *Biochem. Pharmacol.* 2011, *82*, 713–719.

[26] Li, T., Chanda, D., Zhang, Y., Choi, H. S. et al., Glucose stimulates cholesterol 7alpha-hydroxylase gene transcription in human hepatocytes. *J. Lipid Res.* 2010, *51*, 832–842.

[27] Jin, T., Drucker, D. J., Activation of proglucagon gene transcription through a novel promoter element by the caudal-related homeodomain protein cdx-2/3. *Mol. Cell Biol.* 1996, *16*, 19–28.

[28] Janowski, B. A., Grogan, M. J., Jones, S. A., Wisely, G. B. et al., Structural requirements of ligands for the oxysterol liver X receptors LXRalpha and LXRbeta. *Proc. Natl. Acad. Sci. USA* 1999, *96*, 266–271.

[29] DeBlasi, A., O'Reilly, K., Motulsky, H. J., Calculating receptor number from binding experiments using same compound as radioligand and competitor. *Trends Pharmacol. Sci.* 1989, *10*, 227–229.

[30] Li, D., Wang, D., Wang, Y., Ling, W. et al., Adenosine monophosphate-activated protein kinase induces cholesterol efflux from macrophage-derived foam cells and alleviates atherosclerosis in apolipoprotein E-deficient mice. *J. Biol. Chem.* 2010, *285*, 33499–33509.

[31] Veniant, M. M., Sullivan, M. A., Kim, S. K., Ambroziak, P. et al., Defining the atherogenicity of large and small lipoproteins containing apolipoprotein B100. *J. Clin. Invest.* 2000, *106*, 1501–1510.

[32] Chiang, J. Y., Bile acid regulation of gene expression: roles of nuclear hormone receptors. *Endocr. Rev.* 2002, *23*, 443–463.

[33] Gan, X., Kaplan, R., Menke, J. G., MacNaul, K. et al., Dual mechanisms of ABCA1 regulation by geranylgeranyl pyrophosphate. *J. Biol. Chem.* 2001, *276*, 48702–48708.

[34] Wang, Q., Xia, M., Liu, C., Guo, H. et al., Cyanidin-3-O-beta-glucoside inhibits iNOS and COX-2 expression by inducing liver X receptor alpha activation in THP-1 macrophages. *Life Sci.* 2008, *83*, 176–184.

[35] Xia, M., Hou, M., Zhu, H., Ma, J. et al., Anthocyanins induce cholesterol efflux from mouse peritoneal macrophages: the role of the peroxisome proliferator-activated receptor {gamma}-liver X receptor {alpha}-ABCA1 pathway. *J. Biol. Chem.* 2005, *280*, 36792–36801.

[36] Davignon, J., Beneficial cardiovascular pleiotropic effects of statins. *Circulation* 2004, *109*, III39–III43.

[37] Bruckert, E., Giral, P., Tellier, P., Perspectives in cholesterol-lowering therapy: the role of ezetimibe, a new selective inhibitor of intestinal cholesterol absorption. *Circulation* 2003, *107*, 3124–3128.

[38] Mauray, A., Milenkovic, D., Besson, C., Caccia, N. et al., Atheroprotective effects of bilberry extracts in apo E-deficient mice. *J. Agric. Food. Chem.* 2009, *57*, 11106–11111.

[39] Miyazaki, K., Makino, K., Iwadate, E., Deguchi, Y. et al., Anthocyanins from purple sweet potato *Ipomoea batatas* cultivar Ayamurasaki suppress the development of atherosclerotic lesions and both enhancements of oxidative stress and soluble vascular cell adhesion molecule-1 in apolipoprotein E-deficient mice. *J. Agric. Food Chem.* 2008, *56*, 11485–11492.

[40] Miyake, J. H., Duong-Polk, X. T., Taylor, J. M., Du, E. Z. et al., Transgenic expression of cholesterol-7-alpha-hydroxylase prevents atherosclerosis in C57BL/6J mice. *Arterioscler. Thromb. Vasc. Biol.* 2002, *22*, 121–126.

[41] Spady, D. K., Cuthbert, J. A., Willard, M. N., Meidell, R. S., Overexpression of cholesterol 7alpha-hydroxylase (CYP7A) in mice lacking the low density lipoprotein (LDL) receptor gene. LDL transport and plasma LDL concentrations are reduced. *J. Biol. Chem.* 1998, *273*, 126–132.

[42] Erickson, S. K., Lear, S. R., Deane, S., Dubrac, S. et al., Hypercholesterolemia and changes in lipid and bile acid metabolism in male and female cyp7A1-deficient mice. *J. Lipid Res.* 2003, *44*, 1001–1009.

[43] Mauray, A., Felgines, C., Morand, C., Mazur, A. et al., Nutrigenomic analysis of the protective effects of bilberry anthocyanin-rich extract in apo E-deficient mice. *Genes Nutr.* 2010, *5*, 343–353.

[44] Faulds, M. H., Zhao, C., Dahlman-Wright, K., Molecular biology and functional genomics of liver X receptors (LXR) in relationship to metabolic diseases. *Curr. Opin. Pharmacol.* 2010, *10*, 692–697.

[45] Joseph, S. B., McKilligin, E., Pei, L., Watson, M. A. et al., Synthetic LXR ligand inhibits the development of atherosclerosis in mice. *Proc. Natl. Acad. Sci. USA* 2002, *99*, 7604–7609.

[46] Terasaka, N., Hiroshima, A., Koieyama, T., Ubukata, N. et al., T-0901317, a synthetic liver X receptor ligand, inhibits development of atherosclerosis in LDL receptor-deficient mice. *FEBS Lett.* 2003, *536*, 6–11.

[47] Kowalczyk, E., Krzesinski, P., Kura, M., Szmigiel, B. et al., Anthocyanins in medicine. *Pol. J. Pharmacol.* 2003, *55*, 699–702.

[48] Wei, X., Wang, D., Yang, Y., Xia, M. et al., Cyanidin-3-O-beta-glucoside improves obesity and triglyceride metabolism in KK-Ay mice by regulating lipoprotein lipase activity. *J. Sci. Food Agric.* 2011, *91*, 1006–1013.

[49] McGhie, T. K., Walton, M. C., The bioavailability and absorption of anthocyanins: towards a better understanding. *Mol. Nutr. Food Res.* 2007, *51*, 702–713.

[50] Kay, C. D., Aspects of anthocyanin absorption, metabolism and pharmacokinetics in humans. *Nutr. Res. Rev.* 2006, *19*, 137–146.

[51] Crozier, A., Jaganath, I. B., Clifford, M. N., Dietary phenolics: chemistry, bioavailability and effects on health. *Nat. Prod. Rep.* 2009, *26*, 1001–1043.

[52] Frank, T., Netzel, M., Strass, G., Bitsch, R. et al., Bioavailability of anthocyanidin-3-glucosides following consumption of red wine and red grape juice. *Can. J. Physiol. Pharmacol.* 2003, *81*, 423–435.

[53] Scazzocchio, B., Vari, R., Filesi, C., D'Archivio, M. et al., Cyanidin-3-O-beta-glucoside and protocatechuic acid exert insulin-like effects by upregulating PPARgamma activity in human omental adipocytes. *Diabetes* 2011, *60*, 2234–2244.

